Journal of Macromolecular Science, Part A
Publication details, including instructions for authors and subscription information:
http://www.informaworld.com/smpp/title~content=t713597274

A Mechanisms and Kinetics Study of Polymeric Thin-Film Deposition in Glow Discharge

David K. Lam[ab]; Raymond F. Baddour[a]; Arnold F. Stancell[c]
[a] Chemical Engineering Department Massachusetts, Institute of Technology, Cambridge, Massachusetts [b] Xerox Corporation, Webster, New York [c] Mobil Chemical Company, New York, New York

To cite this Article Lam, David K. , Baddour, Raymond F. and Stancell, Arnold F.(1976) 'A Mechanisms and Kinetics Study of Polymeric Thin-Film Deposition in Glow Discharge', Journal of Macromolecular Science, Part A, 10: 3, 421 — 450
To link to this Article: DOI: 10.1080/00222337608061191
URL: http://dx.doi.org/10.1080/00222337608061191

J. MACROMOL. SCI.—CHEM., A10(3), pp. 421-450 (1976)

A Mechanisms and Kinetics Study of Polymeric Thin-Film Deposition in Glow Discharge

DAVID K. LAM* and RAYMOND F. BADDOUR

Chemical Engineering Department
Massachusetts Institute of Technology
Cambridge, Massachusetts 02139

and

ARNOLD F. STANCELL

Mobil Chemical Company
New York, New York 10017

ABSTRACT

Polymeric thin-film deposition in a capacitively coupled rf glow discharge of styrene has been investigated. A kinetic scheme for the polymerization was proposed in which initiation of monomers by electron impact was followed by propagation and termination as in conventional polymerization, the initiation rate constant being a function of electron temperature alone. Four mechanism models were examined, depending on where each reaction step takes place: in the gas phase or on the substrate. Free-radical polymerization was assumed. Experiments were carried out at pressures ranging from 0.25 to 1.05 Torr and at voltages and currents

*Present address: Xerox Corporation, Webster, New York 14580.

that yielded cold and stable discharges. Substrate temperature was controlled. Deposition rate was determined by weighing. A regression program was used in addition to experimental tests in which substrate temperature was varied. The best approximation to the plasma polymer deposition process was found to be the following model: monomers are activated in the gas phase by electron bombardment and subsequently diffuse to the substrate where they propagate and terminate, adsorption of monomers on the substrate playing an important role. A rate expression relating polymer film deposition rate to the experimental variables is presented.

INTRODUCTION

There has been a growing interest in recent years in polymeric thin-film deposition in glow discharge. The research activities are leading to a better understanding of the deposition process and the deposited materials, and important advances in practical applications are being made.

Deposition mechanism proposals have appeared in the literature, and experimental studies on deposition rate variations with variables such as pressure and power have been reported. However, most proposals are qualitative, and, because of the difficulties in interpreting the data, the contribution of the measurements to our understanding of the process has been limited.

Let us consider, for instance, the effects of monomer pressure on deposition rate. An increase in pressure results in the decrease of E/p, the ratio of the electric field intensity to (total) pressure. This in turn leads to decreases in electron temperature T_e and electron concentration. The specific rate constant for initiation k_i, which will be shown to be a sole function of T_e, will also suffer from the lowering of T_e. All of this works to slow down the deposition rate. On the other hand, however, the larger concentration of monomer in the gas phase and a higher level of monomer adsorption on the substrate (provided the substrate is not adsorption-saturated) due to higher monomer pressure will enhance the deposition rate.

Similar difficulty is encountered in interpreting the effects of power on deposition rate. Because voltage and current cannot be independently varied, an increase in power usually results in

increases in both voltage and current, whether the power supply is voltage-regulated or current-regulated. An increase in current may mean higher electron concentration. An increase in voltage can lead to higher E/p and therefore higher k_i and also higher electron concentration. The effects of voltage and current are not readily separable.

Furthermore, as power is increased the gas may heat up, resulting in a higher substrate temperature which can have a pronounced effect on deposition rate [1, 2]. Increase in pressure, too, can lead to higher gas temperature due to increased elastic collision frequency between electrons and molecules, further complicating the interpretation.

In recent years, two attempts [3, 4] have been made to derive a deposition rate expression from a proposed kinetic scheme. The success of these efforts, however, was impaired by, among other factors, their neglect of the important question of mass transport or the vital step of termination in the polymerization reaction.

The purpose of this study is to illucidate the mechanisms and the kinetics of plasma polymer deposition for the case of a vinyl monomer in a vertical plane-parallel electrodes geometry at low monomer flow rate. Experimental data were obtained in "cold" and stable glow discharge conditions.

A kinetic scheme is proposed in which polymer chain termination is included and the reactive species are assumed to be free radicals. Four mechanism models are examined. A steady-state deposition rate expression is developed for each model, taking into account transport mechanisms that bring the molecules from the gas phase to the surface. Empirical parameters in the rate expressions are determined by regression. The models are evaluated by independent experimental tests as well as by comparing their predictions with experimental measurements.

THEORY

The polymerization is assumed to proceed in three consecutive steps: initiation, propagation, and termination. The reactive species are assumed to be free radicals. Initiation of a monomer M is caused by its inelastic collisions with a high-energy free electron e, while propagation and termination are analogous to conventional free radical polymerization [6]. Thus we have

Initiation: $$M + e \xrightarrow{k_i} 2M^{\cdot} + e \quad (1)$$

Propagation: $$M^{\cdot}_x + M \xrightarrow{k_p} M^{\cdot}_{x+1} \quad (2)$$

Termination: $$M^{\cdot}_x + M^{\cdot}_y \xrightarrow{k_t} M_{x+y} \text{ or } M_x + M_y \quad (3)$$

Note that $M^{\cdot}$ represents a molecular fragment of the monomer, and Eq. (1) should be regarded only as a formal representation of the initiation step and not as a true chemical reaction. $M^{\cdot}$ and M may be two very different molecules. For example, the removal of a hydrogen atom from a styrene molecule by electron impact results in the production of two free radicals:

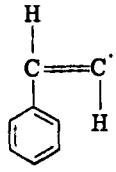

and $H^{\cdot}$

No distinction is made of the two radicals. They are both represented by $M^{\cdot}$ and are both assumed to be potential active centers for polymer chain-propagation.

The specific rate constant k_i for initiation by electron impact can be derived [7] from first principles using gas-kinetic collision theory and the fact that $T_e \gg T_g$ and $m \ll M$, (T_e, T_g being electron and gas temperatures, and m, M the masses of electron and molecule, respectively), if the initiation cross-section σ_i is known. To the extent that σ_i can be assumed to be independent of electron velocity, k_i can be shown to be

$$k_i = \sigma_i(8kT_e/\pi m)^{1/2} \exp(-E_a/kT_e) \quad (4)$$

where E_a is the activation energy for initiation (per molecule) and k the Boltzmann's constant.

Although σ_i, being an inelastic cross-section, is generally a function of the electron energy [8] and unknown for complex molecules, the conclusion remains correct that k_i is a sole function of the electron temperature and T_g is unimportant.

This result can be readily understood from the physical point of view. The specific collision frequency (i.e., collision frequency per molecule per electron) for activation is the product of σ_i and electron velocity. The probability that a colliding electron has an energy equal to or larger than E_a is dependent on T_e for electrons with Maxwell-Boltzmann distribution. k_i is, roughly speaking, the product of the specific frequency and this probability, and should, therefore, depend on T_e alone.

The k_i derived here is for gas-phase initiation. It can be generalized to include polymer molecules as well as monomers.

It can also be shown [8], from the physics of plasmas, that 1) T_e is a function of the ratio E/p, where E is the electric field intensity and p the pressure, although the relation is complicated and unknown, and 2) electron concentration [e] is directly proportional to current density J (current per unit area) and increases with E/p. Thus we have

$$k_i = f_1(E/p) \tag{5}$$

and

$$[e] = Jf_2(E/p) \tag{6}$$

where f_1 and f_2 are unknown functions of E/p.

In light of the kinetic scheme, the various possible mechanisms of deposition can be classified into four distinct cases.

Case 1. Gas-phase initiation, propagation, and termination.
Case 2. Gas-phase initiation and propagation; surface termination.
Case 3. Gas-phase initiation; surface propagation and termination
Case 4. Surface initiation, propagation, and termination.

Because each step can happen in either the gas phase or on the surface, it is necessary to distinguish the concentrations [M] and [M˙] by subscripts i, p, and t in the rate equations r_i, r_p, and r_t for the individual reaction steps.

$$r_i = 1/2k_i[M]_i[e] \tag{7}$$

$$r_p = k_p[M^{\cdot}]_p[M]_p \tag{8}$$

$$r_t = 2k_t[M^{\cdot}]_t^2 \tag{9}$$

Case 1

In this model, monomers are activated in the gas phase. Their subsequent collisions with unactivated monomers lead to chain propagation. The activity of the growing polymers may be annihilated when two of them collide. All of this takes place in the gas phase. But the final products—the terminated polymers—are transported to the substrate where they deposit and make up the polymer film.

Note that $[M]_i = [M]_p = [M]$, and $[M^{\cdot}]_p = [M^{\cdot}]_t = [M^{\cdot}]$ in this case.

In the steady state, $r_i = r_t$, and so

$$[M^{\cdot}] = \{(k_i/4k_t)[M][e]\}^{1/2} \tag{10}$$

Thus the gas-phase polymerization rate R_g is given by

$$R_g = Wr_p = Wk_p[M^{\cdot}][M] \tag{11}$$

where W is average molecular weight of the monomer unit.

The pressure and flow rate in this study were so low that the polymers so formed in the gas phase were transported to the substrate by diffusion alone. Convective transport in the plasma reactor was negligible.

The steady-state diffusion equation for the polymers has $\bar{R}_g$, the average gas-phase polymerization rate, as the constant source function; and one of the boundary conditions states that all polymer molecules reaching the surface will stick and account for the

measured (surface) polymer film growth rate R. The result, after one integration, is simply

$$R = (d/2)\overline{R}_g = (d/2)Wk_p\overline{[M^\cdot]}[M] \tag{12}$$

where d is the electrode separation. [M] is constant in Eq. (12) because there is no consumption of M on the surface, and the polymerization rate in the gas phase is too small to create a gradient. Hence

$$R = (Wd/4)(k_p/k_t^{1/2})\, k_i^{1/2}[M]^{3/2}\overline{[e]}^{1/2} \tag{13}$$

Using Eq. (5) for k_i, Eq. (6) for [e], and the ideal gas law $[M] = p/R_0T_g$, we obtain

$$R = a_1p^{3/2}J^{1/2}F_1 \tag{14}$$

where

$$a_1 = (d/4)[W/(R_0T_g)^{3/2}](k_p/k_t^{1/2}) \tag{15}$$

and

$$F_1 = (f_1f_2)^{1/2} \tag{16}$$

Case 2

In this model, both initiation and chain propagation take place in the gas phase, but the active growing polymers terminate on the substrate to which they diffuse. No propagation is allowed on the surface. So $[M]_i = [M]_p$, but $[M^\cdot]_t \neq [M^\cdot]_p$ since $[M^\cdot]_t$ is a surface concentration and $[M^\cdot]_p$ a volume concentration.

The steady-state diffusion equation for $M^\cdot$ has $\overline{r}_i$, the average initiation rate, as the constant source function; and one of the boundary conditions states that the diffusion flux of $M^\cdot$ must equal the surface termination rate r_t. The results, after one integration, are

$$r_t = (d/2)\bar{r}_i \tag{17}$$

and

$$D_{12}d[M^\cdot]_p/dy + \bar{r}_i y = 0 \tag{18}$$

D_{12} being the diffusivity of $M^\cdot$ in M, and y the space coordinate perpendicular to the electrodes.

Equation (18) has the boundary condition that $[M^\cdot]_p = 0$ at the surface. This is the result of the requirement of the model that an $M^\cdot_p$ (of gas phase propagation) disappear instantaneously and an $M^\cdot_t$ (of surface termination) be born as soon as the former touches the surface. $M^\cdot_p$ and $M^\cdot_t$ are, of course, the same molecule, and $[M^\cdot]_t$ is not zero but is related to $[M^\cdot]_p$ by

$$-D_{12}(d[M^\cdot]_p/dy)_{surface} = 2k_t[M^\cdot]_t^2 \tag{19}$$

The solution of Eq. (18) is

$$[M^\cdot]_p = (\bar{r}_i/2D_{12})[(d/2)^2 - y^2] \tag{20}$$

whose average over the entire space between the elctrodes is

$$\overline{[M^\cdot]_p} = (d^2/12D_{12})\bar{r}_i \tag{21}$$

Recall

$$R = -D_{12}(d[M^\cdot]_p/dy)_{surface}W\bar{x}_n \tag{22}$$

Combining Eq. (22) with Eqs. (18) and (21) at y = d/2, one finds

$$R = (\alpha W d^3/48D_{12})k_p k_i[M]^2[\bar{e}] \tag{23}$$

where $\alpha = \bar{x}_n/\nu$, $\nu = (r_p/r_i)$ = kinetic chain length, and $\bar{x}_n$ = degree

of polymerization. For binary mixtures one can write $D_{12} = B/p$, where B is a constant [9]. Thus

$$R = a_2 p^3 J F_2 \tag{24}$$

where

$$a_2 = (\alpha W d^3/48BR_0^2 T_g^2)k_p \tag{25}$$

and

$$F_2 = f_1 f_2 \tag{26}$$

Case 3

In this model, primary activated monomers are created in the gas phase and then diffuse to the substrate surface where they polymerize with adsorbed monomers. A polymer chain propagates on the surface until its termination. So $[M^\cdot]_t = [M^\cdot]_p$, but $[M]_i \neq [M]_p$ since $[M]_i$ is a volume concentration while $[M]_p$ is a surface one. In the steady state we have $r_t = (d/2)\bar{r}_i$, from which we find

$$[M^\cdot]_t = \{(d/8)(k_i/k_t)[M]_i[\bar{e}]\}^{1/2} \tag{27}$$

$[M]_i$, the gas phase monomer concentration, is constant because the propagation rate (calculated from the measured surface polymerization rate) is far smaller than the monomer random thermal flux at the substrate.

The polymer film growth rate is

$$R = Wr_p = Wk_p[M^\cdot]_p[M]_p \tag{28}$$

So

$$R = W(d/8)^{1/2}(k_p/k_t^{1/2})k_i^{1/2}[M]_i^{1/2}[\bar{e}]^{1/2}[M]_p \tag{29}$$

Note that

$$[M]_i = p/R_0T_g \qquad \text{(moles/cm}^3\text{)} \tag{30}$$

and

$$[M]_p = (A/N_0)\theta(p) \qquad \text{(moles/cm}^2\text{)} \tag{31}$$

where

$\theta(p)$ = fractional coverage of adsorbed monomers on the substrate.
A = number of adsorption sites per unit area.
N_0 = Avogadro's number.

$\theta(p)$, also known as the adsorption isotherm, describes the adsorption behavior of the monomer on the substrate at a given temperature, and is yet to be found. Finally

$$R = a_3 p^{1/2} J^{1/2} \theta F_3 \tag{32}$$

where

$$a_3 = (d/8)^{1/2}(WA/N_0)(R_0T_g)^{-1/2}(k_p/k_t^{1/2}) \tag{33}$$

and

$$F_3 = (f_1 f_2)^{1/2} \tag{34}$$

Case 4

In this model, all three steps of the polymerization take place on the substrate. The most important feature is the assumption that monomers are activated by electron bombardment on the surface. So $[M^\cdot]_t = [M^\cdot]_p$. However, $[M]_i \neq [M]_p$, as will be shown shortly.

The initiation rate r_i is different from the previous three cases. It may be written in terms of the electron bombardment rate $[e]'$ (expressed in, say, number of striking electrons/cm^2/sec), and a cross-section, i.e., probability, k_i' (expressed in, say, cm^2), for the surface initiation. Thus

$$r_i = 1/2k_i'[M]_i[e]' \tag{35}$$

Since the electron flux to the substrate (electrode) is proportional to the measured electric current density, we have $[e]' = \beta J$, where β is a proportionality constant.

Let σ be the geometric cross-section of the target for the impinging electron, S be the fraction of all electrons whose energy E_e is greater than or equal to E_a, and P be the probability that, if $E_e \geq E_a$, a collision leads to a surface initiation. Then the surface initiation cross-section, k_i', is given by

$$k_i' = P\sigma S \tag{36}$$

For electrons with a Maxwell-Boltzmann velocity distribution, S can be shown to be [10]

$$S = 1 - \text{erf}(Z) + (2/\pi^{1/2})Z \exp(-Z^2) \tag{37}$$

where

$$Z = (E_a/kT_e)^{1/2}$$

Thus it can be seen that k_i' is again a function of T_e alone, and we can write, by analogy with k_i,

$$k_i' = f_3(E/p) \tag{38}$$

Note that the impinging electron will hit either an adsorbed monomer or a monomer unit in a surface polymer chain. So if k_i' is assumed to be applicable to activating a monomer unit as well as an adsorbed monomer, the effective $[M]_i$ is constant and given by $[M]_i = A/N_0$.

On the other hand, $[M]_p$, for the propagation step, is not constant but is determined by the adsorption isotherm, as in Eq. (31). Now, in the steady state, $r_i = r_t$. So

$$[M^{\cdot}]_p = \{(k_i'/4k_t)[M]_i[e]'\}^{1/2} \tag{39}$$

Thus

$$R = a_4 J^{1/2} \theta F_4 \tag{40}$$

where

$$a_4 = (W/2)\beta^{1/2}(A/N_0)^{3/2}(k_p/k_t^{1/2}) \tag{41}$$

and

$$F_4 = f_3^{1/2} \tag{42}$$

For physical adsorption of styrene and its fragments, the BET equation [11] was used, and

$$\theta(x) = cx/(1 - x)[1 + (c - 1)x] \tag{43}$$

where c is an empirical constant, and $x = p/p_0$, p_0 being the saturated monomer vapor pressure at the prevailing temperature.

Preliminary experiments also showed that R varied approximately linearly with E/p. Thus the F-functions may be adequately represented by a simple power law

$$F(E/p) = b(E/p)^n \tag{44}$$

where b and n are empirical constants.

The functional dependence of R on p, J, E/p, and x for all four cases are summed up in Table 1. The empirical constants to be determined are (a,n) for Rate Expressions 1 and 2, and (a,n,c) for Rate Expressions 3 and 4, a being a new proportionality constant of the rate expressions.

EXPERIMENTAL

Rf power was capacitively coupled to the discharge through a pair of vertical parallel-plate internal electrodes. Pressure, voltage, and current were measured. Substrate temperature was maintained at 20°C except when variation of adsorption was intended.

The apparatus consisted of the deposition cell, the sampling system, the vacuum and monomer feed system, the rf generation and measurement units, and the electrode-cooling system. Description of these parts and the methods of measurement are given below.

TABLE 1. Functional Dependence of Polymer Deposition Rate

Model	Initiation	Propagation	Termination	Functional dependence of R
1	Gas	Gas	Gas	$p^{3/2}J^{1/2}(E/p)^n$
2	Gas	Gas	Surface	$p^3J(E/p)^n$
3	Gas	Surface	Surface	$p^{1/2}J^{1/2}(E/p)^n\{cx/(1-x)[1+(c-1)x]\}$
4	Surface	Surface	Surface	$J^{1/2}(E/p)^n\{cx/(1-x)[1+(c-1)x]\}$

The deposition cell (Fig. 1) consisted of 1) a 100-cm^2 square brass electrode and a square stainless steel electrode of the same size that is water-cooled, 2) Teflon electrode guards to prevent the edges and the back of the electrodes from exposure to the gas, 3) Teflon spacers to maintain a constant separation of 2.2 cm

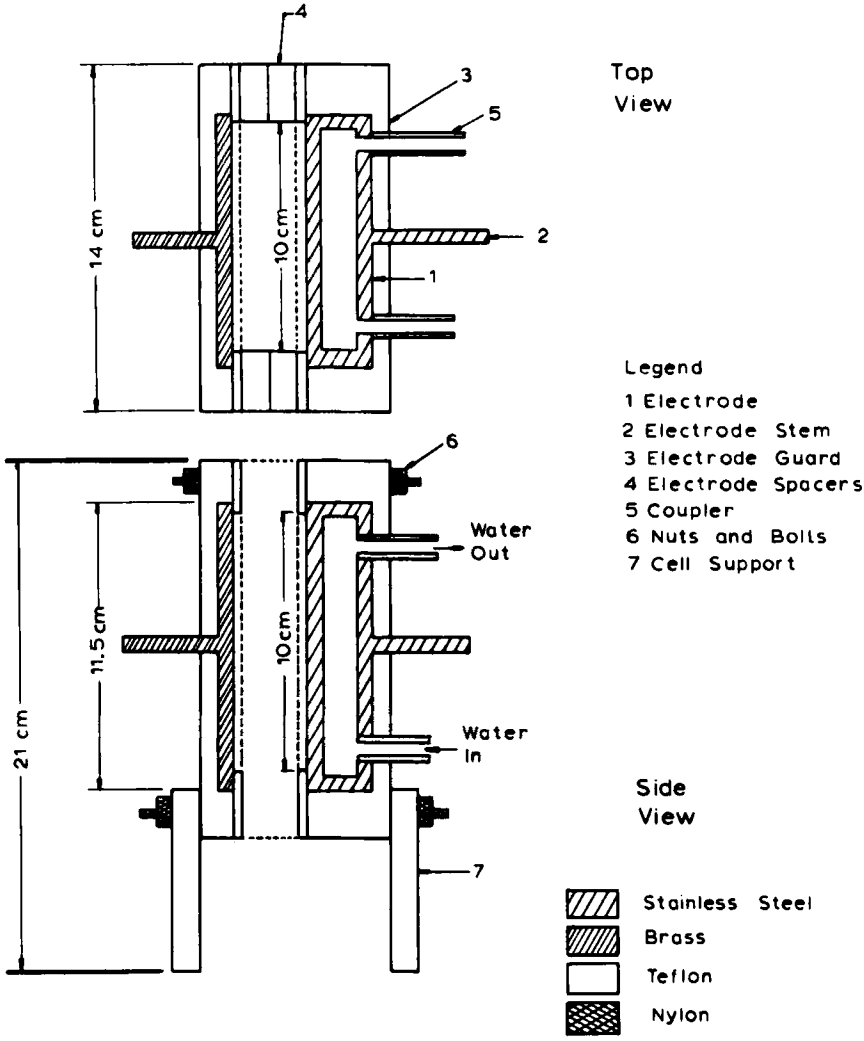

FIG. 1. Deposition cell.

between the electrodes, and 4) Teflon cell supports to raise the cell assembly to an appropriate height.

The spacers were only placed on the two sides, so the cell had openings on the top and the bottom for vertical downward gas flow. The cell was bolted together with nylon threaded rods and nuts at four corners, and sat on the baseplate of the vacuum chamber more or less on top of the pumping port.

The two electrode stems were connected to the terminals of the power generator; one to the high voltage terminal, the other through a known low-value resistor to the rf ground.

The sample holder (Fig. 2) was a stainless steel bracket with a pocket into which the sampling slide was snugly placed. The sample holder was itself snugly mounted on and had good electrical and thermal contacts with the water-cooled electrode. Thus the slide and the holder could be considered as being at the same electrical potential and the same temperature as the electrode.

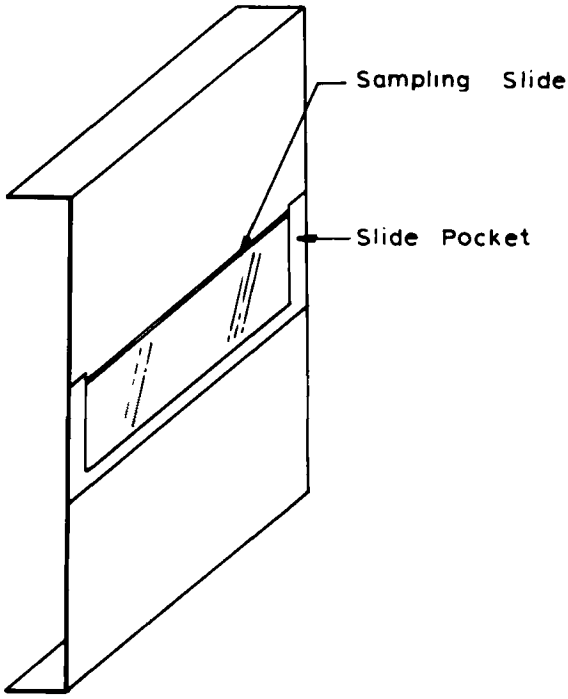

FIG. 2. Sample holder.

The sampling slides were cut from 5-mil thick stainless steel shim stock. Each of them had a constant area of 10.6 cm^2 exposed to the glow discharge when it rested in the sample holder.

The amount of polymer deposited on the slide was determined by weighing, using a Sartorius Balance (Satorius-Werke AG, Type 1801) which could be read to 1 μg.

The vacuum system consisted of a 12-in. bell-jar (the deposition chamber), a diffusion pump, a liquid nitrogen cold trap, and a large rotary oil pump. An ionization gauge and a thermocouple gauge were used to monitor pressure at pumpdown.

Monomer pressure in the chamber was measured by a Baratron differential pressure transducer, manufactured by MKS Instruments Inc., Burlington, Massachusetts, Model 77M-XR-2, which was accurate to 1 mμ. The reference pressure was maintained at 0.001 Torr.

The deposition cell was located near the center of the chamber, about 4 in. above the baseplate. Electrical power and cooling water were brought to the electrodes via feedthroughs in the baseplate.

Styrene monomer vapor was drawn from a liquid reservoir at room temperature through a rotameter and metering valves and, via a feedthrough at the baseplate, to the top of the deposition chamber. The styrene, supplied by Eastman Kodak Co., Rochester, New York, Stock No. 1465, and stabilized with tert-butylpyrocatechol with normal boiling point stated to be between 33 to 35°C, was used as received. The monomer vapor was not diluted; argon was only used for purging the system.

A schematic of the apparatus is shown in Fig. 3, which omits details of the deposition cell assembly and the cooling system.

The electrical power needed to sustain the glow discharge was generated by a Lepel rf induction heating unit, manufactured by Lepel High Frequency Laboratories, Inc., New York, New York, Model T-2.5B, with a maximum power output of 2.5 kW. This unit was only made for inductive-coupling arrangement, but voltage could be tapped off from the work-coil (the induction coil surrounding the object to be heated). This voltage was then brought to one of the electrodes (the high-voltage electrode) by coaxial cables. The unit was designed to oscillate at 450 kHz. But the dimensions and turn-number of the work-coil that was installed changed its resonance frequency to 800 kHz. All data were obtained at 800 kHz.

One electrode was maintained at several hundred volts at 800 kHz, while the other at essentially ground potential. Voltage measurements were made at Point A (Fig. 3). Current was monitored at Point B (Fig. 3) by inserting an accurately measured (1 Ω) high-frequency resistor R between the "ground" electrode and the rf ground.

Voltage and current were measured with a Tektronic probe (Type P6017) and were displayed on a high impedance (1 MΩ), high frequency (up to 10 MHz) Telequiment oscilloscope (Type S54). The

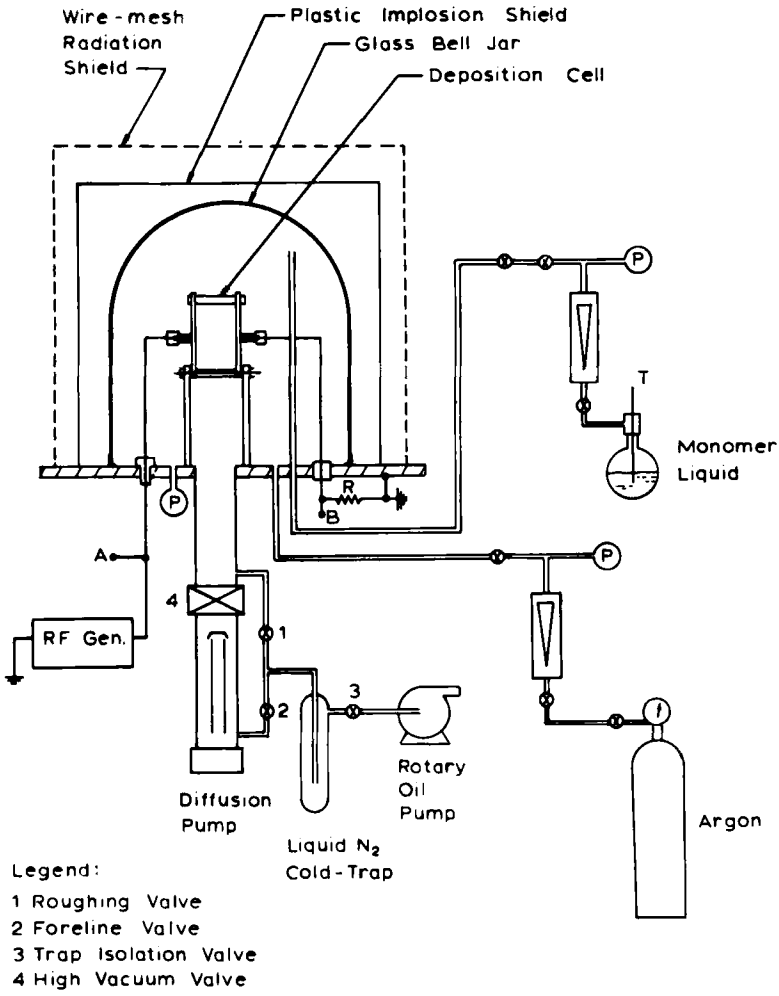

FIG. 3. Schematic of apparatus (details of deposition cell assembly and electrode cooling system not shown).

peak-voltage rating of the oscilloscope was 400 V and of the probe 600 V. So the voltage to be measured (which peaked at around 400 V) was reduced by a factor of 10 by a calibrated voltage divider.

The high-voltage electrode was maintained at a constant temperature of 20°C by circulating water to and from a thermostatted water bath. In order to prevent current leakage through the cooling water

to the ground, which could result in short-circuiting and loss of power, the following measures were taken:

1. The inside of the water-cooled electrode was coated with a layer of Rust-Oleum paint.
2. Distilled water was used whose electrical conductivity was measured to be two orders of magnitude lower than that of city water.
3. An IR lamp, placed outside against the stainless steel water tank, was used for heating. The tank was thermally insulated with asbestos except for the area exposed to the lamp.
4. A glass, instead of metal, condenser was used to cool the tank water; water circulating in the condenser was chilled by ice.
5. A magnetic pump was used to circulate the water. The water was electrically insulated from the pump itself, which was grounded.
6. The metallic stirrer in the tank was electrically isolated, by using a short section of nylon rod, from the grounded motor that drove it.
7. The temperature-sensing probe of the Thermistemp temperature controller was spray-coated with several layers of Krylon plastic.

The cooling water flow rate was 1.3 gal/min, and the temperature in the bath was maintained at 20°C to an accuracy of ±0.05°C.

The deposition chamber was pumped down to 10^{-3} Torr or lower for some 30 min before the high vacuum valve was closed, the diffusion pump heater turned off, leaving only the cold trap and the mechanical pump operative, and the monomer vapor admitted to the deposition chamber at a fixed feed rate setting (3×10^{-5} mole/min or 0.7 STP cc/min). The pressure in the chamber was allowed to rise to a predetermined level, and was kept there by controlling the pumping speed with the roughing and the cold-trap isolation valves.

When pressure, flow rate, and substrate temperature had all been stabilized for 10 to 20 min, the rf power was turned on to initiate the discharge. The power was adjusted to bring about some low voltage level sufficient to sustain a stable glow discharge. A momentary high voltage was needed at the start to insure gas breakdown in some runs.

The pressure always dropped slightly, and valve settings were readjusted to bring back the original value.

Peak to peak voltage was measured on the oscilloscope, from which the rms voltage was calculated. The current waveform was always somewhat distorted from a pure sinusoid, so its average

value must be obtained by graphical integration of the waveform. The current reading was repeated six or seven times (approximately 10 min apart) during each 1-hr run. These values were later plotted against the time at which they were recorded. A smooth curve was drawn through them, and the mean value obtained from graphical integration was the reported current. This value, in general, was almost identical to the arithmetic mean of the several current readings.

The phase angle between voltage and current could also be checked using the oscilloscope, and it was always zero within limits of experimental errors.

At the end of the 60-min run, the sampling slide was removed from the deposition cell and stored in air for 24 hr before being weighed again.

RESULTS, ANALYSES, AND DISCUSSION

Because the rate expressions were formulated for steady-state conditions, it was imperative that the experimental data were also obtained in steady-state. Figure 4 shows the polymer weight collected on the sampling slide as a function of deposition time, up to 1-1/2 hr, at one operating condition. The linear relationship was evident, within limits of experimental error (see Appendix), and the straight line passed through the origin, indicating that the deposition rate virtually reached steady-state instantaneously. The result is also in agreement with most other observations reported in the literature [2-5].

In order to obtain a reasonable amount of polymer deposit, however, all experiments were run for exactly 1 hr.

In each experiment, pressure p, voltage V, current I, and the polymer weight W_p on the sampling slide were measured. Substrate temperature T_s was assumed to be the same as the coolant temperature which was maintained constant at 20°C. Results are shown in Table 2.

Because of the limited cooling capacity, the assumption on T_s is good only if the heat flux from the gas to the electrode is small. Large heat flux will occur if the gas temperature T_g in the glow discharge is much higher than T_s. Therefore, the discharge must be "cold," i.e., T_g must <u>not</u> be far from room temperature.

There was another important reason. If the gas was hot, the polymer deposition on the electrode would be grossly nonuniform, with the center where the sampling slide was located and where

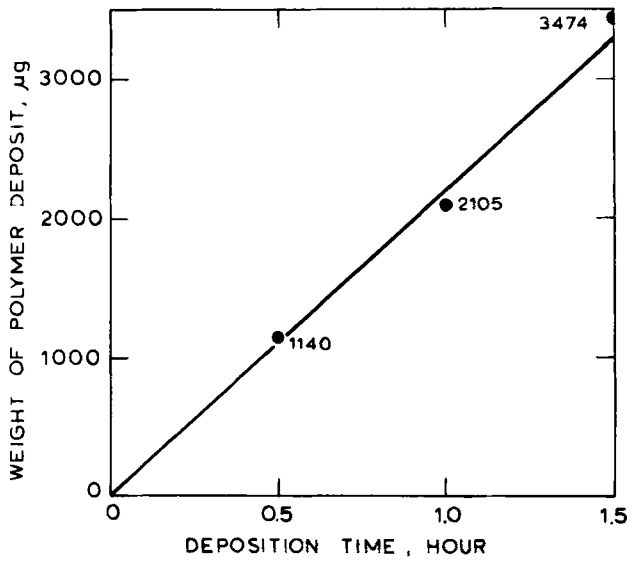

FIG. 4. Polymer weight vs deposition time: p = 0.55 Torr, V = 410 volt, I = 118 mA.

TABLE 2. Experimental Data

p (Torr)	V (V)	I (mA)	W_p (μg)	R ($\mu g/cm^2$-min)
0.25	459	71	1388	2.18
0.35	434	83	1569	2.47
0.45	406	90	1920	3.02
0.55	413	115	2010	3.16
0.65	396	110	2187	3.44
0.75	396	124	2532	3.98
0.85	336	69	1593	2.50
0.95	385	163	2851	4.48
1.05	330	53	1435	2.26

the temperature was higher relative to the upper and lower edges, having the least deposition, resulting in a meaningless polymer weight measurement.

While a glow discharge could be sustained over a range of voltages for a given pressure, a "cold" discharge could be obtained only when the operating voltage was near the lower end of the range. This also meant low current since current could not be separately varied. The resulting discharge was quite stable as long as it was not near extinction. In the low pressure runs, the glow was so weak that it was not visible unless the room was sufficiently dark.

All the experimental data that were used to evaluate the models were obtained under cold and stable discharge conditions.

The discharge became unstable at 0.15 Torr pressure and lower, and the gas was too easy to heat up at pressures higher than 1.05 Torr. With reduced voltage, cold discharge could be obtained at pressures somewhat higher than 1.05 Torr. But at such low voltages, the current was found too small to be accurately measured. Hence operating pressure ranged from 0.25 to 1.05 Torr. The pressure limits could, of course, be shifted up or down if the electrode gap was allowed to vary. The electrode separation, however, was held constant at 2.2 cm in this study.

The styrene vapor feed rate in the experiments was kept at 0.75 STP cc/min, a fraction of which flowed through the deposition cell, while the remainder by-passed it and was pumped out. The relative importance of the two modes of mass transport in the cell, diffusion and convection, could be estimated using the heat transfer analogy. In other words, one could use the Sherwood number, Sh: if $Sh \gg 1$, convection is the predominant mode; if $Sh \ll 1$, diffusion dominates over convection [12]. Calculations showed that, under the conditions in this study, Sh was no greater than 0.03, the upper limit corresponding to the assumption that all monomer vapor passed through the cell. The assumption in the rate expressions, that activated species and polymer molecules reached the substrates by diffusion alone, appeared to be valid.

The polymer films adhered well to the sampling slide, appeared hard, smooth, and yellow, and were 1.3 to 2.7 μm thick. They were not soluble in toluene, benzene, or styrene. No powder was found in the film under proper operating conditions. Small amounts of white powder polymer could be observed, at higher pressures and voltages, to flow out of the bottom of the deposition cell toward the pumping port. But the amount could be reduced by operating the glow discharge at lower voltages and currents. The fact that the slide as well as the electrodes were vertical also helped prevent most powders from accumulating in the sample.

As pointed out earlier, voltage and current could not be varied independent of each other. This was partly due to an inherent

voltage-current relation of the plasma and partly due to the circuitry of the power supply. In any event, this limitation, plus the requirement of cold and stable discharge conditions, made it impossible to obtain deposition data by systematically varying any one of the variables (p, V, I, and x) over a wide range while holding the others constant. The data, given in Table 2, had to be analyzed with the aid of a computer program for multiparameter nonlinear regression.

The regression analysis involved minimization of the differences between the computed and the experimental deposition rates to determine the parameters in the rate expressions. Once the "best" set of parameters was obtained, the difference between the rate predicted by the model and the rate measured was to be examined in the light of the permissible experimental errors.

To evaluate each rate expression, the program required a set of initial values of the parameters to be determined, which was obtained by precursory calculations. A polymer deposition rate R_{th} was then computed for each set of (p, V, I, and x), and compared to the measured deposition rate R (Column 5, Table 2). A percentage difference δ, defined as $\delta = [(R_{th} - R)/R] \times 100$, was obtained for each data point. The sum of the squares of all the δ's was to be minimized as the program searched for a better set of parameters.

From Table 1, the rate expressions for the four models can also be written as follows.

Rate Expression 1:

$$R = ap^{3/2}I^{1/2}(V/p)^n \tag{45}$$

Rate Expression 2:

$$R = ap^3I(V/p)^n \tag{46}$$

Rate Expression 3:

$$R = ap^{1/2}I^{1/2}(V/p)^n\{cx/(1 - x)[1 + (c - 1)x]\} \tag{47}$$

Rate Expression 4:

$$R = aI^{1/2}(V/p)^n\{cx/(1 - x)[1 + (c - 1)x]\} \tag{48}$$

where V and I have replaced E and J, respectively, which will alter the values of a by a constant factor, but will not affect c or n.

J and I are related by the defining relation $J = I/A_e$, where A_e is the electrode area. On the other hand, the relation $E = V/d$, where d is the electrode gap, does not hold in the discharge since E is not spatially constant. In particular, at the gas-solid interface, where a "sheath" develops and where electrical neutrality no longer holds, the electric field intensity there can be orders of magnitude higher than that in the bulk of the discharge where E is constant and low. However, the thickness of the sheath is small, extending only a fraction of a millimeter from the electrode surface under the prevailing discharge conditions. Furthermore, as a result of ambipolar diffusion, which was expected to prevail, electron concentration drops from its maximum at the midplane to zero at the electrode surface. Thus the effect of a large E in the sheath may be counterbalanced to a great extent by the lack of electrons there, leaving the bulk of the discharge being the effective reaction medium. Nevertheless, V was assumed to be proportional to E in the bulk, although the proportionality constant need not be d.

The final set of parameters corresponding to the minimum sum of δ^2's are given in Table 3, for each rate expression, which also shows $|\delta_{max}|$ and δ_{rms}, the largest and the root-mean-square δ.

The limits of experimental errors were found to be typically ±9.5% (see error analysis in Appendix). It can be seen that only Models 3 and 4 have their values of $|\delta_{max}|$ smaller than the

TABLE 3. Regression Analysis Results

Rate expressions (model)	Parameters[a]			Percentage difference	
	a $\times 10^3$	n	c	$\lvert\delta_{max}\rvert$	δ_{rms}
1	5.0	0.75	-	32	20
2	0.80	0.70	-	92	58
3	5.5	0.70	19	7.8	4.7
4	15	0.58	5.5	8.1	4.9

[a]Parameter values are to be used in Eqs. (45) through (48) with p in Torr, I in mA, V in volt (rms), and R in $\mu g/cm^2$-min.

experimental errors allowed for in the measurements. Models 1 and 2 were thus considered as incorrect representations of the polymer deposition process because they failed to satisfy the criterion.

The failure of Models 1 and 2 was consistent with experimental observations in this study (see below) and in the literature, that adsorption plays an important role in the deposition process, at least for the case of deposition on the electrodes. Neither of Rate Expressions 1 and 2 could account for adsorption effects. On the other hand, the regression analysis does not distinguish between the two remaining expressions.

If one now examines Rate Expressions 3 and 4, one will find a large difference in their sensitivity to x: percentage increments of θ with x in Rate Expression 4 are considerably larger than that in Rate Expression 3. This difference permits further experimental tests in which only x is varied, to determine which one of the expressions can better describe the polymer deposition process.

If T_s, which has heretofore been maintained at 20°C, is varied, the change in R should correspond to the change in adsorption since p, V, and I all remain constant. In other words, R_{T_s}/R_{20} should be the same as θ_{T_s}/θ_{20}.

The results of three experiments, in which T_s was lowered to 16°C and raised to 24°C at two difference pressures, are given in Table 4, which also shows predictions from Rate Expressions 3 and 4. It is evident that Rate Expression 3 predicts consistently and significantly better than Rate Expression 4. It was concluded, therefore, that Model 3 can best describe the polymer deposition process in glow discharge, and the deposition rate can be represented by

TABLE 4. Results of Adsorption Test on Models 3 and 4[a]

T_s (°C)	p_o (Torr)	p (Torr)	R_{T_s}/R_{20}	θ_{T_s}/θ_{20} Model 3	θ_{T_s}/θ_{20} Model 4
16	4.5	0.45	1.13	1.12	1.22
16	4.5	0.65	1.08	1.11	1.21
24	7.0	0.45	0.97	0.91	0.85

[a]At 0.45 Torr, V = 406 volts and I = 87 ± 5 mA. At 0.65 Torr, V = 396 volts and I = 117 ± 7 mA.

$$R = 5.5 \times 10^{-3} p^{1/2} I^{1/2} (V/p)^{0.70} [19x/(1 - x)(1 + 18x)] \quad (49)$$

where p is in Torr, I in mA, V in volts (rms), $x = p/p_0$, and R in $\mu g/cm^2$-min. Thus activated species are primarily created in the gas phase, and propagation as well as termination takes place on the substrate with adsorbed monomers taking an important part.

Initiation by visible and UV radiations, electron and ion bombardments of, and electron-ion recombinations on the substrate are known to be possible. Their contribution, however, is believed to be small in comparison to gas-phase initiation by electron impact under the weak-glow, low-voltage, and low-current discharge conditions in this study.

Activated monomers may also start chain propagation in the gas phase before they can reach the substrate by diffusion. But the contribution to the total propagation rate is not expected to be significant since the number of molecular mean-free-paths from the midplane to either electrode was only in the order of 300.

Free radicals can be trapped in the polymer as the film grows, thereby providing an additional mechanism of termination. This will enhance the chain-termination rate, leading to a higher effective k_t and a lower deposition rate. The form of the rate expression, however, was not affected.

Equation (49) can also be written as

$$R = 5.5 \times 10^{-3} I^{1/2} V^{0.70} G(p) \quad (50)$$

where

$$G(p) = 19\, p^{0.80}/(p_0 - p)(p_0 + 18p) \quad (51)$$

Here, G(p) accounts for all pressure effects on R. When G(p) is plotted against p at constant p_0 corresponding to 20°C for styrene (i.e., 5.75 Torr), the curve, shown in Fig. 5, is reminiscent of the many observations on variations of R with p reported in the literature.

The deposition rate is directly proportional to k_p, as can be seen from Eqs. (32) and (33). One might wonder whether a change in T_s as in the adsorption tests would not have an effect on k_p also, since propagation takes place on the substrate.

If one assumes the activation energy of propagation E_p obtained from conventional free-radical polymerization to be valid, a drop

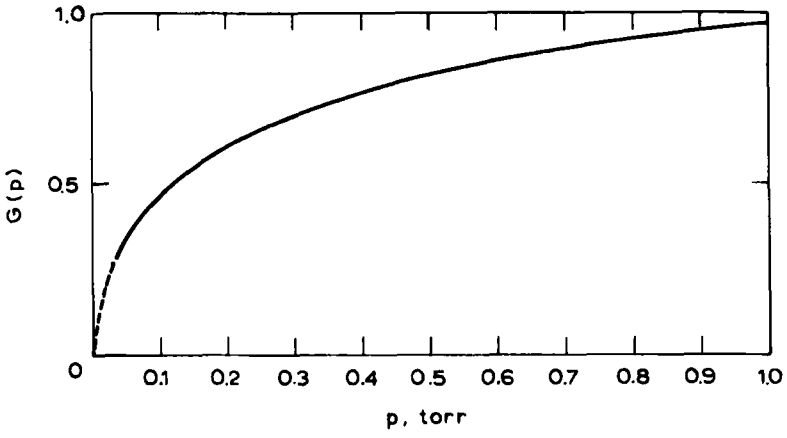

FIG. 5. G(p) vs p.

in T_s would have resulted in a corresponding decrease in the reaction rate. In contrast, however, this study as well as all published results on glow discharge polymerization indicated that that was not the case.

For example, E_p for styrene free-radical polymerization is known to be about 7.8 kcal/mole [6]. Simple calculation shows that a drop of 4°C from 20°C would have led to an 18% decrease in the deposition rate, if this value of E_p were valid. The measured rate change, as we recall, was instead an increase of 13% and was consistent with the adsorption behavior.

Interestingly, an adsorption effect very similar to that observed in glow discharge polymerization has also been well known in polymerization by UV photolysis [13] and by electron bombardment [14].

The reason for the observed discrepancy is that the Arrhenius-type kinetics can be violated in plasma chemical reactions [15] and other chemical reactions where excitation of molecules and/or nonequilibrium occur. The breakdown of the classical Arrhenius kinetics is due to two of its basic assumptions that all internal degrees of freedom of the molecules can be ignored and that all reactants are at thermal equilibrium at a unique temperature.

We have already seen one violation of the Arrhenius kinetics earlier when the specific initiation rate constant k_i was shown to be independent of gas temperature, and only dependent on electron temperature. That was an example in which the reactants (electrons on the one hand, and ions and molecules on the other) were not in thermal equilibrium.

More important, and perhaps less obvious, however, is the fact that a specific reaction rate constant is a function of not only the translational temperature, but also the rotational, the vibrational, and the electronic temperatures of the reactants. For example, a rate constant may depend upon the concentrations of molecules in certain quantum states. In glow discharge polymerization where a substantial fraction of the molecules are in various excited states, an activation energy, such as E_p, obtained in an Arrhenius plot from an equilibrium reaction, is not expected to apply.

Many adsorbed monomers on the substrate were vibrationally as well as rotationally excited. Although they were not activated in the sense that they themselves became active centers for chain growth, their excess internal energies had largely overcome the energy barrier that might exist in the propagation step. As a result, changes of translational energy of the adsorbed monomers, due to substrate temperature variations, had little effect on k_p.

APPENDIX

The method is presented which was used to arrive at the limits of experimental errors permitted in the comparison of the computed rate R_{th} using a rate expression, and the experimentally measured rate, called R_{exp} here. The word error is synonymous to uncertainty.

If the rate expression is expressed in terms of generalized exponents l, m, and n, then

$$R = ap^l J^m (E/p)^n \theta(x) \tag{A-1}$$

which can also be written as

$$R = ap^{l'} J^m E^n \theta(x) \tag{A-2}$$

where

$$l' = l - n \tag{A-3}$$

Then, by partial differentiation, one finds

$$\frac{dR}{R} = l' \frac{dp}{p} + m\frac{dJ}{J} + n\frac{dE}{E} + \left(\frac{\partial R}{\partial \theta}\right) \frac{d\theta}{\theta} \tag{A-4}$$

Also, differentiating

$$\theta(x) = cx/(1 - x)[1 + (c - 1)x] \tag{A-5}$$

with respect to x and rearranging, we obtain

$$d\theta/\theta = [1 + (2 + 2/c)\theta x]\ (dx/x) \tag{A-6}$$

If we assumed no errors in p_0, then

$$dx/x = dp/p \tag{A-7}$$

and

$$d\theta/\theta = [1 + (2 + 2/c)\theta x]\ (dp/p) \tag{A-8}$$

Thus the percentage error in θ depends on c, x, and θ itself, as well as the percentage error in p. For large c (say, $c > 10$), Eq. (A-8) may be approximated by

$$d\theta/\theta \simeq (1 + 2\theta x)\ (dp/p) \tag{A-9}$$

Noting $(\partial R/\partial\theta) = 1$, $dJ/J = dI/I$, and $dE/E = dV/V$, and substituting Eq. (A-8) in Eq. (A-4), we obtain the "worse-case" estimate of the uncertainty in R_{th} due to experimental uncertainties in p, V, and I.

$$\left|\frac{dR}{R}\right| = \left|1'\frac{dp}{p}\right| + \left|m\frac{dI}{I}\right| + \left|n\frac{dV}{V}\right| + \left|[1 + (2 + 2/c)\theta x]\ \frac{dp}{p}\right| \tag{A-10}$$

Maximum, minimum, and "typical" percentage errors in p, V, I, and R_{exp} are summed up in Table 5.

When R_{th} is compared to R_{exp}, as in the evaluation of the models, the percentage error that can be allowed for is the sum of the calculated percentage error of R_{th} (using Eq. A-10) and the experimental error in R_{exp} (from Table 5).

TABLE 5. Percentage Errors in p, V, I, and R_{exp}

Variable	Percentage error		
	Maximum	Minimum	"Typical"
p	1.2 (low p)	0.4 (high p)	0.8
V[a]	6.4 (low V)	5.2 (high V)	5.8
I	6.0	4.0	5.0
R_{exp}	1.7 (low R_{exp})	1.3 (high R_{exp})	1.5

[a]Except for $V_{rms} > 440$ volt where uncertainty could be as high as 9.7% due to a change to a coarser scale. The voltage itself, however, was very stable at high V_{rms}.

Example

Rate Expression 3 is given by

$$R = 5.5 \times 10^{-3} p^{1/2} I^{1/2} (V/p)^{0.70} [19x/(1 - x)(1 + 18x)] \quad (49)$$

From Eq. (A-10) we have

$$|dR/R| = (1.2 + 2.1\theta x)|dp/p| + 0.50|dI/I| + 0.70|dV/V|$$

θx varies from 0.02 to 0.18, so we will take 0.1 as the representative value. If we also take the typical percentage errors for p, V, and I from Table 5, we obtain

$$\text{Error in } R_{th} = 1.4 \times 0.8\% + 0.5 \times 5\% + 0.7 \times 5.8\%$$

$$= 7.7\%$$

Again from Table 5, the typical error in R_{exp} is 1.5%. So in comparing R_{th} with R_{exp}, a difference of (7.7 + 1.5)%, or 9.2%, may be allowed.

ACKNOWLEDGMENTS

This work was supported by the National Science Foundation. We also thank Halcon International, Inc., New York, for a graduate fellowship to one of us (D.K.L.). Helpful and stimulating discussions with Professor Paul J. Flory and Mr. James D. Dearth are gratefully acknowledged.

REFERENCES

[1] T. Williams and M. W. Hayes, Nature, 209, 769 (1966).
[2] A. R. Westwood, Eur. Polym. J., 7, 363 (1971).
[3] A. R. Denaro, P. A. Owens, and A. Crawshaw, Ibid., 4, 93 (1968).
[4] H. Yasuda and C. E. Lamaze, J. Appl. Polym. Sci., 15, 2277 (1971).
[5] M. L. Vasile and G. Smolinsky, J. Electrochem. Soc., 119, 453 (1972).
[6] P. J. Flory, Principles of Polymer Chemistry, Cornell Univ. Press, Ithaca, New York, 1953.
[7] V. N. Kondrat'ev, Chemical Kinetics of Gas Reactions (translated by J. M. Crabtree and S. N. Carruthers), Pergamon, Oxford, 1964, pp. 138-147.
[8] S. C. Brown, Introduction to Electrical Discharges in Gases, Wiley, New York, 1966.
[9] R. B. Brid, W. E. Stewart, and E. N. Lightfoot, Transport Phenomena, Wiley, New York, 1960, p. 505.
[10] F. W. Sears, Thermodynamics, The Kinetic Theory of Gases, and Statistical Mechanics, 2nd ed., Addison-Wesley, Reading, Massachusetts, 1953, p. 239.
[11] J. M. Thomas and W. J. Thomas, Introduction to the Principles of Heterogeneous Catalysis, Academic, London, 1967.
[12] E. R. G. Eckert and R. M. Drake, Jr., Heat and Mass Transfer, 2nd ed., McGraw-Hill, New York, 1959.
[13] P. White, Microelectron. Reliab., 2, 161 (1963).
[14] R. W. Christy, J. Appl. Phys., 31, 1680 (1960).
[15] L. Polak, "Some Principles of Nonequilibrium Plasma-Chemical Reaction Kinetics," in Reactions under Plasma Conditions, Vol. 2 (M. Venugopolan, ed.), Wiley, New York, 1971.